Photonic Entanglement Based on Nonlinear Metamaterials

Yang Ming,* Wang Zhang, Jie Tang, Yuan Liu, Zilong Xia, Yushen Liu,* and Yan-qing Lu*

Metamaterials consisting of deep subwavelength artificial "atoms" have been utilized to demonstrate a series of novel phenomena such as negative refraction and epsilon-near-zero. In recent times, metamaterials have been developed as an up-and-coming platform for quantum optics. Here the generation and modulation of photonic entanglement are investigated based on the parametric down conversion processes in metamaterials with considerable optical nonlinearity. Through flexible nanostructure design, the nonlinear photonic interaction in the metamaterial system can be effectively tailored. The distributions of optical parameters of the system are inhomogeneous, based on which the spatial properties of the generated photonic state can be steered as desired. The theoretical framework to describe this system is established based on the nonlinear Huygens–Fresnel principle, and a differential approach is utilized to deal with the intrinsic loss of the system. The generation of orbital angular momentum entangled states is actually considered as an illustration. This platform could be valuable for the practical applications of quantum information processing.

1. Introduction

Metamaterials are engineered structures with unique electromagnetic properties and functionalities which are not attainable with naturally existing materials.[1] More recently, owing to the high designability and flexibility, metamaterials have been deeply studied and exploited for novel photonic applications such as negative refraction, near-zero permittivity, and wavefront shaping.[2–6] There are various sorts of photonic metamaterials. A typical sort is the ones with structural units consisting of dielectric or metallic subwavelength building blocks known as the artificial "atoms."[7,8] Accordingly, the light-matter interaction properties of the metamaterials can be tailored by modulating the resonance of "meta-atoms" through material selection and geometry design, or arranging their distributions and orientations in space.[1] The value of this characteristic has been thoroughly demonstrated in classical optics. Moreover, it could play an important role in the context of quantum photonics. Especially, recent explorations of nonlinear optical metamaterials[9] provide a potential platform for generating and manipulating entangled photon states,[10–12] which are at the heart of quantum information processing.

The development of quantum physics presents intriguing novel concepts inexhaustibly, which brings excellent opportunities to cut down the time-complexity of quantum algorithms.[13] Correspondingly, the arithmetic capability is greatly improved in theory. However, the practicality of photonic quantum computation usually requires multiparticle systems. With the increasing of photon number, the efficiency and operability of the systems face enormous challenges. As an alternative, multidimensional systems can be exploited for certain quantum information applications.[14] The spatial degrees of freedom of photon provide potential candidates, which can be used to form infinite dimensional Hilbert space.[15] Compared with hyperbolic metamaterials[16,17] and negative-index "meta-waveguides,"[18,19] the meta-atom constructing systems provides an ideal platform to steer the spatial properties of photonic states owing to the abundant and flexible micro/nano-structures. Several investigations taking advantage of this unique characteristic have been demonstrated.[20–22] However, so far the twin photons are generated prior to the interaction with metamaterials in most cases. In this letter article, we study utilizing nonlinear metamaterials for directly generating entangled photon states with expected characteristics. Such kind of function integration could be benefit for reducing the complexity of practical systems. Through designing and arranging of meta-atoms, the parametric down conversion (PDC) processes inside the nonlinear metamaterials can be controlled to effectively engineer the entangled states. For an exact description of such a system, a theoretical framework is developed based on the combination of the nonlinear Huygens–Fresnel principle and the equivalent beam splitter approach for attenuation. The generation of entangled orbital angular momentum (OAM) states is actually considered and calculated to be available. The nonlinear metamaterials provide a potential platform for steering photonic entanglement.

Dr. Y. Ming, Z. Xia, Prof. Y. Liu
School of Physics and Electronic Engineering
Changshu Institute of Technology
Suzhou 215000, China
E-mail: njumingyang@gmail.com; ysliu@cslg.edu.cn
Dr. Y. Ming, W. Zhang, J. Tang, Y. Liu, Prof. Y.-q. Lu
National Laboratory of Solid State Microstructures, College of Engineering and Applied Sciences
Nanjing University
Nanjing 210093, China
E-mail: yqlu@nju.edu.cn

The ORCID identification number(s) for the author(s) of this article can be found under https://doi.org/10.1002/lpor.201900146
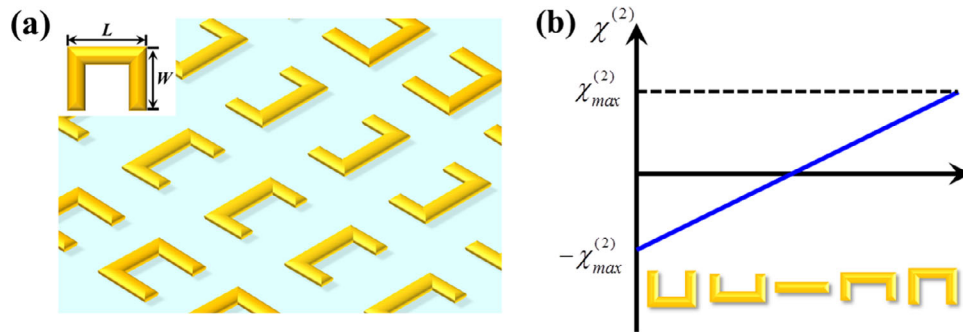
Figure 1. a) The schematic of the SRR-based nonlinear metamaterials. The insert exhibits the geometry of SRR meta-atom. b) The absolute value of $\chi_{max}^{(2)}$ varies with the length L and width W of the meta-atom, and the sign of $\chi_{max}^{(2)}$ depends on the orientation of the meta-atom.

2. Results and Discussion

2.1. Tuning the PDC Process with Nonlinear Metamaterials

Traditionally, entangled photons are generated through multiphoton interaction processes.[4] The dynamical process is controlled by the interaction Hamiltonian whose formalism is directly influenced by the nanostructures of the nonlinear metamaterials. Therefore, Hamiltonian engineering can be realized through nanostructure design. Correspondingly, the PDC process can be steered to generate photonic state on demand.

For actual metamaterials, there are various kinds of meta-atoms such as split ring resonator (SRR)[23] and nanoantenna with N-fold rotational symmetry.[24] The modulation of photonic states can be realized through tuning the shape and orientation of the meta-atoms. In the present work, we consider a SRR array system as is shown in **Figure 1**a, and the geometry of SRR meta-atom is presented in the inset.

Compared with the traditional domain-engineered ferroelectric nonlinear crystals, the distribution of nonlinear coefficient of the SRR system can experience a continuous variation through changing the geometry of SRR meta-atom.[23] As is shown in Figure 1b, the absolute value of local nonlinear coefficient of a meta-atom can be modulated between 0 and a maximum $\chi_{max}^{(2)}$ through tuning the ratio between the length of the SRR arm and the total effective length of the SRR. In addition, the sign of nonlinear coefficient depends on the orientation of the meta-atom. Owing to the current powerful nano-fabrication technologies, the shape, orientation, and distribution of SRR meta-atoms can be tailored on demand. Correspondingly, such a system provides a more accurate platform for controlling the spatial properties of entangled photon states than the binary modulation regime of the ferroelectric nonlinear crystals based on the inversion of polarization direction.

To clarify the mechanism of PDC in SRR system, the conventional quasi-phase matching regime is not adequate owing to the structural complexity, thus a more generalized theoretical framework needs to be established. Therefore, we introduce the nonlinear Huygens–Fresnel principle.[25] That is to say, in PDC process, each point on the wavefront of the pump light acts as a sub-source of secondary down-converting waves through interacting with nonlinear metamaterials. The influence of each point source could be expressed with the Hamiltonian density as[26]

$$\mathcal{H}_I(\vec{r}) = \frac{1}{2}\hat{P}_{NM}(\vec{r}) \cdot \hat{E}_p(\vec{r})$$

$$= \frac{1}{2}\chi_{NM}^{(2)}(\vec{r})\hat{E}_p^{(+)}(\vec{r})\hat{E}_s^{(-)}(\vec{r})\hat{E}_i^{(-)}(\vec{r}) \tag{1}$$

In this equation, the subscripts p, s, and i represent the pump, signal, and idler photons, respectively. The nonlinear coefficient of metamaterial medium is marked as $\chi_{NM}^{(2)}$. The pump field E_p is usually treated as an undepleted classical field. The signal and idler fields are quantized and represented by field operators. The corresponding expressions are written as

$$E_p^{(+)} = E_{p0}\Psi_{pt}(\vec{r})e^{i(\vec{k}_p \cdot \vec{r} - \omega_p t)}$$

$$E_s^{(-)} = i\sum_\sigma \int d\omega_s \int d\vec{k}_s F_{s\sigma}\Psi_{st}(\vec{r})a_{s\sigma}^\dagger e^{-i(\vec{k}_s \cdot \vec{r} - \omega_s t)}$$

$$E_i^{(-)} = i\sum_\sigma \int d\omega_i \int d\vec{k}_i F_{i\sigma}\Psi_{it}(\vec{r})a_{i\sigma}^\dagger e^{-i(\vec{k}_i \cdot \vec{r} - \omega_i t)} \tag{2}$$

The pump light is set to be monochromatic, and E_{p0} is the corresponding amplitude, while the function $\Psi_{pt}(\vec{r})$ represents the transverse shape. $F_{s(i)\sigma}$ is the normalization parameter. Furthermore, $\Psi_{st}(\vec{r})$ and $\Psi_{it}(\vec{r})$ describe the transverse distributions of the signal and idler photons, including the amplitude and phase profile. In addition, $a_{s(i)}^\dagger$ is the creation operator for the signal (idler) field. The polarization state of the signal (idler) photons is marked by the parameter σ.

The contribution of a point source in the generated photon state could be evaluated with the evolution equation as $|d\Psi\rangle = [1 - (i/\hbar)\int dt\mathcal{H}_I(t)]|0\rangle$. The final down-converted state can be derived through summing the contributions over the whole volume of nonlinear metamaterial. For a quasi two dimensional (2D) system in which the nonlinear metamaterial is a thin slice, it is not hard to obtain the form of the two-photon state with the spatial integral of $|d\Psi\rangle$ as

$$|\Psi\rangle_t = \int d\vec{r}\,|d\Psi\rangle$$

$$= |0\rangle + \frac{iE_{p0}}{2\hbar}\sum_{\sigma,\sigma'}\int d\vec{k}_s \int d\vec{k}_i F_{s\sigma}F_{i\sigma'}$$

$$\times \Theta(\vec{k}_s, \vec{k}_i)a_{s\sigma}^\dagger a_{i\sigma'}^\dagger |0\rangle \tag{3}$$
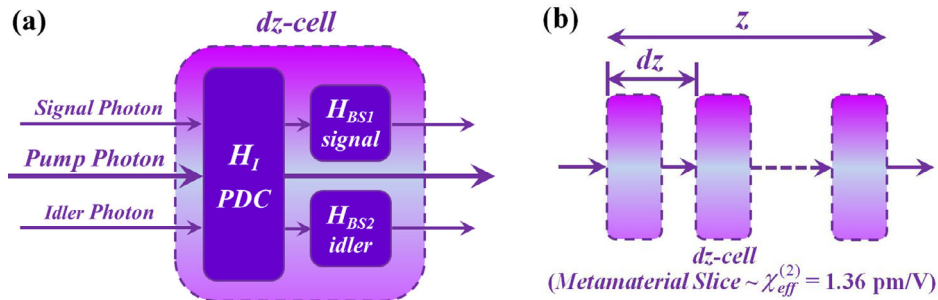
Figure 2. The illustration of the PDC process in nonlinear metamaterials. a) Detailed configuration of a *dz*-cell. The PDC process in a *dz* element is divided into two sub-processes. The interaction of pump, signal, and idler photons is assumed to be locally lossless, and the effective nonlinear susceptibility is $\chi_{\text{eff}}^{(2)} = 1.36$ pm V^{-1}. The influence of pump loss can be covered with the varying pump amplitude $A_p(z)$ including in the form of Hamiltonian. The losses of the down-converted photons are equivalent to two beam splitter transformation, respectively. b) The final output state could be derived through cascading all *dz*-cells.

with

$$\Theta(\vec{k}_s, \vec{k}_i) = \int d\vec{r} \chi_{\text{NM}}^{(2)}(\vec{r})\Psi_{pt}(\vec{r})\Psi_{st}(\vec{r})\Psi_{it}(\vec{r})$$

$$\times e^{i(\vec{k}_p - \vec{k}_s - \vec{k}_i)\cdot\vec{r}}\delta(\omega_p - \omega_s(\vec{k}_s) - \omega_i(\vec{k}_i)). \quad (4)$$

From the function $\Theta(\vec{k}_s, \vec{k}_i)$, it could be clearly seen that the spatial properties of the generated state are determined by the pump light and the nanostructures of the nonlinear metamaterials. Correspondingly, the entangled photon states can be tailored through flexible design of the metamaterials.

If we consider more complicated systems, that is, three dimensional (3D) nonlinear metamaterials, the situation is relatively difficult to deal with. In view of the structural complexity, an available approach to prepare 3D nonlinear metamaterials is stacking 2D metamaterial slices.[27,28] Such systems are chosen to be discussed in the present work. The longitudinal direction is set to be perpendicular to the slices, while the transverse section is parallel to them. In principle, there are several crucial issues that should be taken into account in these multilayered structures, including reflection, transmission, and absorption of the waves in each metamaterial layer.[29] These issues make the wave dynamics in such nonlinear multilayered metamaterials become a complication to solve. However, the problem can be simplified in certain circumstances. For dielectric substrates with small meta-atoms, the reflection of the layers is relatively low. Correspondingly, we could neglect that and consider only the absorption caused by metallic components in the metamaterial system to obtain analysis results. Several methods are usually utilized to deal with absorption in quantum systems, such as the Liouvillian formulation,[30] the Green function,[17,31] and the equivalent beam splitter model.[32–34] According to the geometric character of the stacking system, it is relatively convenient to take advantage of the third method together with a differential approach in which the entire interaction medium is divided into a series of differential elements along the longitudinal direction. A 2D slice naturally plays as a *dz*-element. This model is reasonable for a system with low losses, which also requires that the meta-atoms are tiny. For metamaterials with large SRRs, the power of light decreases drastically when passing through the multilayer structure. Nevertheless, the transmittance can obtain a definite improvement as

the duty cycle and volume of meta-atom reducing.[29] Several previous investigations have demonstrated that the transmittance of SRR layer can reach a high level under ideal circumstances,[35,36] which is crucial for keeping the theoretical model working well.

The intrinsic loss makes it impossible to define a global Hamiltonian for the SRR system. However, that is not a problem for the differential model. In each *dz*-element, the lossy nonlinear interaction process could be equivalently compartmentalized into two cascaded sub-processes. For the first sub-process, the decay is separated out, thus a local lossless Hamiltonian can be defined to describe the interaction; for the second sub-process, the attenuation is calculated with a beam splitter transformation. The final results can be obtained through combining all these *dz*-elements in sequence. The total processes are illustrated in **Figure 2**.

As is shown in Figure 2a, a *dz*-element is regarded as a cell. The three-photon interaction is described by the Hamiltonian based on Equations (1) and (2). The attenuation of the signal and idler photons is represented by the corresponding beam splitter transformation with effective Hamiltonian as

$$H_{\text{BS}}(z) = \sum_\sigma \int d\omega_s \sqrt{2\gamma_s} \left[a_{s\sigma} b_{s\sigma}^\dagger(z) + a_{s\sigma}^\dagger b_{s\sigma}(z) \right]$$

$$+ \sum_{\sigma'} \int d\omega_i \sqrt{2\gamma_i} \left[a_{i\sigma'} b_{i\sigma'}^\dagger(z) + a_{i\sigma'}^\dagger b_{i\sigma'}(z) \right] \quad (5)$$

In the equation above, the operator $b_{s(i)}^\dagger(z)$ describes the loss of a photon at coordinate z, and $\gamma_{s(i)}$ is the corresponding attenuation coefficient.

A cell describes the operations of a metamaterial slice acting on its input state. To achieve the target photonic state, we should carefully design each cell and suitably arrange them, which is illustrated in Figure 2b. In the simplest case, if the pump light is assumed to be undepleted (In low loss systems, such an approximation is usually reasonable) and all the metamaterial slices have identical nanostructures, the interaction Hamiltonian should be *z*-independent. Otherwise, the cells are inhomogeneous. Moreover, when the decay of the pump light is considered, the influence of attenuation can be covered with the varying pump amplitude $A_p(z)$ including in the form of Hamiltonian. Based on the discussions above, the evolution of state vector in nonlinear metamaterials can be expressed as[33,37,38]
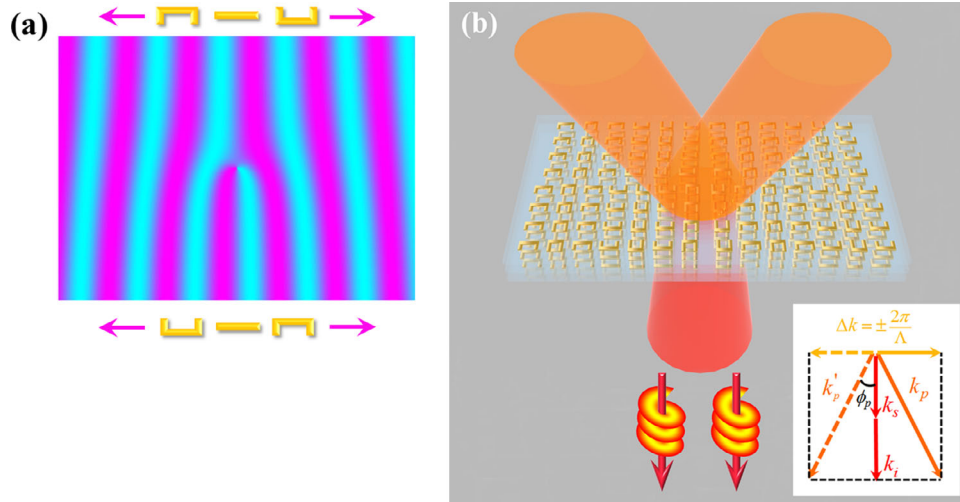
Figure 3. a) The spatial distribution of nonlinear coefficient $\chi^{(2)}$ of the fork-shaped metamaterials. b) The illustration of PDC process in the nonlinear metamaterial. The geometric regime of photon interaction is shown in the inset.

$$\begin{aligned} |\Psi(z)\rangle = {} & \frac{iE_{p0}}{2\hbar} \sum_{\sigma,\sigma'} F_{s\sigma} F_{i\sigma'} \Theta(z) a_{s\sigma}^\dagger a_{i\sigma'}^\dagger |0\rangle \\ & + \sum_{\sigma,\sigma'} \left[\int_0^z dz_1 \Theta_s(z, z_1) a_{s\sigma}^\dagger b_{i\sigma'}^\dagger(z_1) |0\rangle \right. \\ & \left. + \int_0^z dz_1 \Theta_i(z, z_1) b_{s\sigma}^\dagger(z_1) a_{i\sigma'}^\dagger |0\rangle \right] \\ & + \sum_{\sigma,\sigma'} \int_0^z dz_{ls} \int_0^z dz_{li} \Theta_{si}(z_{ls}, z_{li}) b_{s\sigma}^\dagger(z_{ls}) b_{i\sigma'}^\dagger(z_{li}) |0\rangle \end{aligned} \tag{6}$$

with

$$\begin{aligned} \frac{\partial \Theta(z)}{\partial z} = {} & -i\hbar \left[\omega_p - \frac{2(\gamma_s + \gamma_i)}{E_{p0} F_{s\sigma} F_{i\sigma'}} \right] \Theta(z) \\ & + \frac{iE_{p0}}{2\hbar} F_{s\sigma} F_{i\sigma'} I_{psi} \chi_{NM}^{(2)}(z) A_p(z) \end{aligned}$$

$$\frac{\partial \Theta_s(z, z_1)}{\partial z} = -(i\hbar\omega_s + \gamma_s)\Theta_s(z, z_1), \quad z \geq z_1$$

$$\frac{\partial \Theta_i(z, z_1)}{\partial z} = -(i\hbar\omega_i + \gamma_i)\Theta_i(z, z_1), \quad z \geq z_1$$

$$\Theta_{si}(z_{ls}, z_{li}) = \begin{cases} -i\frac{1}{2}\sqrt{2\gamma_s}\Theta_s(z_{ls}, z_{li}), & z_{ls} \geq z_{li} \\ -i\frac{1}{2}\sqrt{2\gamma_i}\Theta_i(z_{li}, z_{ls}), & z_{ls} \leq z_{li} \end{cases} \tag{7}$$

In Equation (6), the first term corresponds to the biphoton state without considering attenuation, while the second and third terms describe the loss of signal and idler photons, respectively. The corresponding position is marked as z_1. The last term represents the simultaneous loss of both signal and idler photons.

With these theories, arbitrary photon state with desired properties can be achieved through suitable design of the medium in

an ideal situation. This is of great practical value for quantum photonic applications. In the next section, we would discuss the generation of OAM entangled state with nonlinear metamaterials in detail.

2.2. Generation of OAM Entangled State with Fork-Shaped Metamaterials

The OAM of photon is explicitly defined by L. Allen et al. in 1992.[39] It is related to the helical phase term $\exp(il\theta)$. The parameter l can be any integer number, and it is defined as the topological charge, which indicates that each corresponding photon possesses an OAM of $l\hbar$. Owing to the unique features of OAM, it has attracted a lot of research interest in recent years. For quantum information processing, as a high-dimensional Hilbert space can be defined based on the OAM degree of freedom,[40] it is extremely valuable for information capacity expansion. However, for the reason of spatial complexity, it is usually not easy to construct OAM entangled photon states. The designability of nonlinear metamaterial system makes it an ideal platform to accomplish this task.

In the area of linear optics, a special diffraction element known as fork grating is usually used to generate optical vortex carrying OAM.[41] In the present work, we introduce this structure into the nonlinear metamaterial system. For the metamaterial slices, the substrates are chosen to be silica, while the SRR meta-atoms consist of gold. The orientations of the meta-atoms on a single slice are carefully arranged to present a fork-shaped distribution. The corresponding spatial variable nonlinear coefficient $\chi^{(2)}$ is shown **Figure 3**a. In this situation, the expression of $\chi^{(2)}$ can be written as

$$\chi_{NM}^{(2)}(\vec{r}) = \chi_{max}^{(2)} \cos\left[2\pi \frac{x}{\Lambda} + l_{NM}\theta \right] \tag{8}$$

In the equation above, Λ is defined as the modulation period in the x direction, while l_{NM} is the equivalent topological

**ADVANCED
SCIENCE NEWS**

www.advancedsciencenews.com

**LASER
& PHOTONICS
REVIEWS**

www.lpr-journal.org

charge of the metamaterial slice. In addition, the azimuthal coordinate is defined as $\theta = \tan^{-1}(y/x)$. As we consider the generation of OAM entangled state, the transverse profile functions $\Psi_{st}(\vec{r})$ and $\Psi_{it}(\vec{r})$ should be set as $\exp(il_s\theta)$ and $\exp(il_i\theta)$. The pump light is chosen to be TEM$_{00}$ Gaussian beam as $E_p(\vec{r}) = E_{p0} \times \exp\{-[(x\cos\phi_p - z\sin\phi_p)^2 + y^2]/\delta_0^2\} \times \exp(i\vec{k}_p \cdot \vec{r} + il_p\theta)$ where ϕ_p is the input angle of the pump light and δ_0 is the beam waist. Substituting these expressions together with Equation (8) into Equation (3), we could obtain the state vector of down-converted photons as

$$|\Psi\rangle_t = |0\rangle + \frac{iE_{p0}\chi_{max}^{(2)}}{4\hbar} \sum_{\pm 1} \sum_{\sigma,\sigma'} \int d\vec{k}_s \int d\vec{k}_i \int d\vec{r}$$

$$\times F_{s\sigma}F_{i\sigma'}e^{-[(x\cos\phi_p - z\sin\phi_p)^2 + y^2]/\delta_0^2}$$

$$\times e^{\pm i2\pi\frac{x}{\Lambda}}e^{i(\vec{k}_p - \vec{k}_s - \vec{k}_i)\cdot\vec{r}}$$

$$\times e^{i(l_p \pm l_{NM} - l_s - l_i)\theta}a_{s\sigma}^{\dagger}a_{i\sigma'}^{\dagger}|0\rangle \quad (9)$$

In this equation, as the higher-order Fourier components of $\chi^{(2)}$ are eliminated, we could see that there are only two cases marked as ± 1 order. Compared to the ferroelectric crystal system with multi-diffraction order,[26] this characteristic is highly beneficial for assuring the purity and generation efficiency of target OAM modes. According to the phase term $e^{\pm i2\pi\frac{x}{\Lambda}}e^{i(\vec{k}_p - \vec{k}_s - \vec{k}_i)\cdot\vec{r}}$, the pump light is chosen to be obliquely launched on the metamaterial to ensure the conservation of linear momentum. Moreover, to simplify the situation, the propagation directions of the signal and idler photons are set to be along the z axis, thus we have

$$k_p\sin\phi_p = \pm\frac{2\pi}{\Lambda}$$
$$k_p\cos\phi_p = k_s + k_i \quad (10)$$

As is shown in Figure 3b, when the input direction is tilted along the positive x axis, the OAM should satisfy $l_s + l_i = l_p + l_{NM}$ based on the conservation law. In contrast, if the pump light is launched from another side, the conservation of OAM writes as $l_s + l_i = l_p - l_{NM}$. Under such circumstances, the generated OAM entangled state could be expressed as

$$|\Psi\rangle_t = \sum_{l_s, l_i} F_{l_s, l_i}|l_s\rangle|l_i\rangle \quad (11)$$

The coefficient F_{l_s,l_i} could be derived through the approach of Schmidt decomposition.[42] As the azimuthal modes automatically satisfy the requirement of Schmidt eigenvectors,[43] F_{l_s,l_i} are the corresponding natural Schmidt eigenvalue.

Owing to the condition Equation (10), the oscillating exponential phase factor is eliminated, so it is not necessary to introduce in z-dependent spatial variations along the longitudinal direction to ensure the transformation efficiency. For simplification, we just consider stacking identical 2D metamaterial slices in the present system. To obtain an explicit understanding, we do the calculations of the PDC process based on a practical system. The pump wavelength is set at 0.6 µm. The entanglement is restricted to the degenerate case where the wavelength of the signal and

idler photons are both chosen to be 1.2 µm. In this situation, the attenuations of the two down-converted photons are identical. According to the discussions in the last section, OAM doses not affect the damping process, thus the influences of the intrinsic loss of nonlinear metamaterials act on the photon pairs equally. As a result, the effect of decay on the quantum properties of the OAM entangled state can be ignored in our system. The only distinction compared with the lossless system is that the generation efficiency is drawn down. Consequently, the analyses and calculations are greatly simplified.

For concrete parameters, the geometry of meta-atom is set as $L = 100$ nm and $W = 80$ nm, and the gap between two meta-atoms is 150 nm. With Equation (10), the input angle of the pump light should be $\phi_p = 6.7°$, thus the period Λ is 5.12 µm. The effective thickness of a single slice in the multilayered structure is 50 nm. In this situation, the theoretical attenuation rate of signal and idler photons is calculated to be $\alpha_{s/i} = 1.06 \times 10^3$ m^{-1}. It is worth mentioning that the intrinsic loss owing to the metallic components of metamaterials is not quite large in deed. In actual systems, the insertion loss always brings a negative impact to some extent. Nevertheless, for the degenerate case, the corresponding influence on the signal and idler photons is symmetrical, thus the analytical regime is not seriously hampered. Although the calculated generation efficiency is expected to exceed reality, it can still provide important reference values. The polarization of the pump light should be parallel to the xz plane according to the response characteristics of SRR. The value of $\chi_{max}^{(2)}$ is difficult to evaluate exactly in theory, so the only reliable access is measurement. According to previously reported investigations, the result is $\chi^{(2)} \approx 1–100$ pm V^{-1}.[44] For fundamental reference, we take a conservative value 1.36 pm V^{-1} from ref. [23]. Correspondingly, the generation efficiency of entangled photons is calculated with different values of pump power and layer number in the case of $l_p = 0$ and $l_{NM} = 1$, as is shown in **Figure 4**a. In Figure 4b,c, we plot the coincidence probabilities $|F_{l_s, l_i}|^2$ as a function of l_s and l_i for ($l_s = 0$; $l_{NM} = 1$) and ($l_p = 1$; $l_{NM} = 2$). In actual systems, the situation could be better. With a $\chi^{(2)}$ of ten several units, the PDC efficiency can reach $\approx 10^{-15}$. As the effective element of nonlinear coefficient is d_{22} (≈ 2 pm V^{-1}) in the ferroelectric system based on lithium niobate crystals,[26] the efficiency of SRR system is expected to be not worse under otherwise equal conditions. For practical considerations, a femtosecond laser can be chosen as the pump source, which is widely used in studying the nonlinearity of photonic metamaterials. If the laser parameters are 2 µJ per pulse and 250 fs, the production rate of photon-pair can approach 10^{-1} per pulse when the transformation efficiency is in the magnitude of 10^{-15}, which is available for practical applications.[45,46] With a beam spot of 150 µm diameter, the power intensity is lower than 0.1 TW cm^{-2}, which is still safe for metallic metamaterials to avoid damage of melting.[47]

As regards the general non-degenerate entanglement system, the calculations should be done in accordance with specific conditions. If the wavelengths of down-converted photons are close, the situation does not significantly deviate from the degenerate case. Therefore, the properties of the OAM entangled state are not affected basically. However, that surely brings limit to the generation rate of entangled photon pairs. The corresponding level
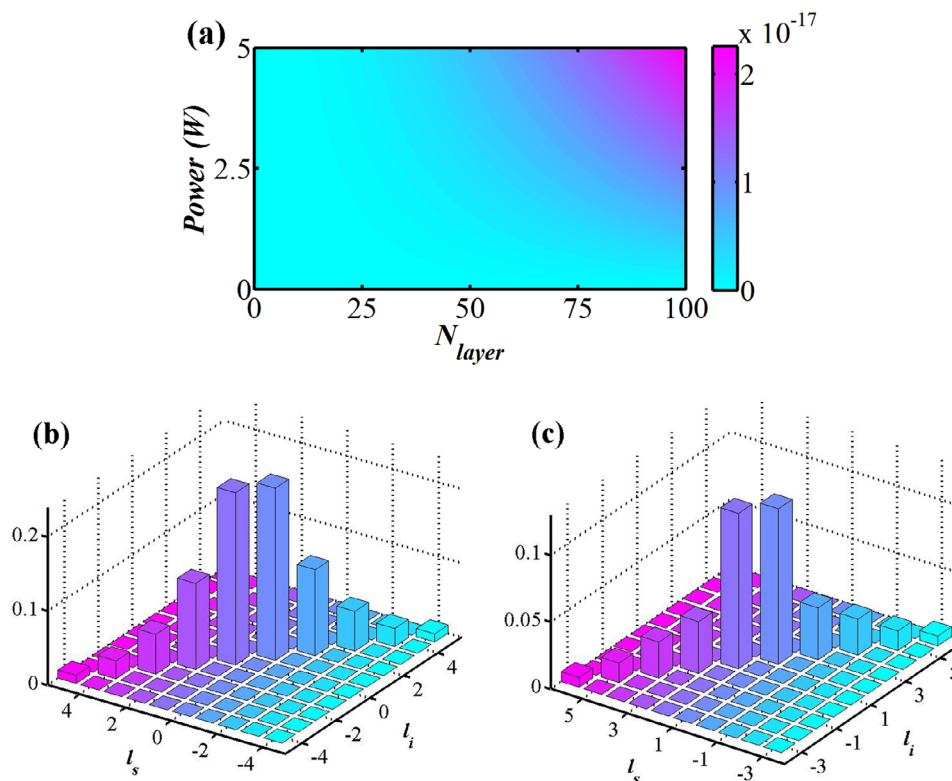
**ADVANCED
SCIENCE NEWS**

www.advancedsciencenews.com

**LASER
& PHOTONICS
REVIEWS**

www.lpr-journal.org

Figure 4. a) The generation efficiency of entangled photons correspond to different values of pump power and layer number when we have $l_p = 0$ and $l_{NM} = 1$. The coincidence probabilities as a function of l_s and l_i for b) $l_p = 0$ and $l_{NM} = 1$ and c) $l_p = 1$ and $l_{NM} = 2$ are plotted.

depends on multiple factors, such as the fabricating technologies of metamaterials and the working wavelength. For the deep non-degenerate case, such limit becomes much more momentous. Not only does the generation rate reduce, but also the degree of entanglement is cut down. In near-infrared region, the influence may be not extremely massive owing to the relatively small dispersion. Beyond this situation, it is necessary to take effective means to purify entanglement. Metamaterials can also be used for this task.[48,49]

To propose an experimental system, the common coincidence measurement can still be considered.[50] However, it is a challenge to prepare multilayered nonlinear metamaterial samples. This does not prevent the effort to explore available fabricating technologies because metamaterials really provide an ideal platform for controlling light-matter interaction which is also of great value in quantum information applications. Based on the traditional electron beam lithography, the fabrication of meta-materials with ten several layers is available.[51] For more layers, it is indeed difficult to keep the perfect quality, yet there are still improved technologies such as nanoimprint lithography[52] and femtosecond laser-induced forward-transfer technique[53] providing opportunities. Moreover, other solutions can also be considered. If several metamaterial samples are cascaded, the interaction region will be lengthened. Nevertheless, they should be carefully arranged to avoid additional insertion loss to the most extent. Furthermore, the cavity is also an alternative choice, and the optical path should be well set to protect the spatial properties of photonic states.[54]

3. Conclusion

The development of quantum photonic technologies sheds new light on the future applications of optics and information science. As the crucial physical resource, entangled photons are traditionally explored in the area of multi-photon entanglement for practical utilizations. However, the generation efficiency of the corresponding states usually decreases with a rise of photon number,[55] which brings wide-ranging restrictions. As an alternative, photonic entanglement in the spatial degrees of freedom could provide another choice in certain situations based on the multi-dimensional Hilbert space. Previously, the ferroelectric-based nonlinear photonic crystals are utilized for tailoring the spatial properties of entangled states,[26] but there are limits in two aspects, that is, fineness and scale of the structures. The size of structural units can easily reach submicron level for SRR system while that is several microns or more for domain-engineered ferroelectric crystals. The meta-atoms prepared through processing technologies such as electron-beam lithography is common to be in the scale of several hundred nanometers. An associated advantage is that the whole scale of metamaterial samples is usually smaller than that of ferroelectric crystals, which is meaningful for the integration of photonic quantum circuits. These features make nonlinear metamaterials a better platform for tailoring the spatial properties of photonic states with higher accuracy and flexibility.

In summary, we investigate generating photonic entanglement with special spatial properties based on the PDC process

in nonlinear metamaterials. Combing the nonlinear Huygens–Fresnel principle and propagation damping theories, the analytical framework is established. Through nanostructure design, a fork-shaped metamaterial is proposed, based on which OAM entangled photons could be effectively generated. This platform can be further extended for applications as quantum interference,[56,57] Purcell enhancement,[16,58] and coherent perfect absorption.[59,60]

Conflict of Interest

The authors declare no conflict of interest.

[1] N. Engheta, R. W. Ziolkowski, *Metamaterials: Physics and Engineering Explorations*, Wiley-IEEE Press, New York **2006**.

[2] D. R. Smith, J. B. Pendry, M. C. K. Wiltshire, *Science* **2004**, *305*, 788.

[3] J. Valentine, S. Zhang, T. Zentgraf, E. Ulin-Avila, D. A. Genov, G. Bartal, X. Zhang, *Nature* **2008**, *455*, 376.

[4] K. Hur, Y. Francescato, V. Giannini, S. A. Maier, R. G. Hennig, U. Wiesner, *Angew. Chem., Int. Ed.* **2011**, *50*, 11985.

[5] R. Maas, J. Parsons, N. Engheta, A. Polman, *Nat. Photonics* **2013**, *7*, 907.

[6] I. Dolev, I. Epstein, A. Arie, *Phys. Rev. Lett.* **2012**, *109*, 203903.

[7] Y. F. Yu, A. Y. Zhu, R. Paniagua-Domínguez, Y. H. Fu, B. Luk'yanchuk, A. I. Kuznetsov, *Laser Photonics Rev.* **2015**, *9*, 412.

[8] X. Zheng, W. Smith, J. Jackson, B. Moran, H. Cui, D. Chen, J. Ye, N. Fang, N. Rodriguez, T. Weisgraber, C. M. Spadaccini, *Nat. Mater.* **2016**, *15*, 1100.

[9] M. Lapine, I. V. Shadrivov, Y. S. Kivshar, *Rev. Mod. Phys.* **2014**, *86*, 1093.

[10] M. Siomau, A. A. Kamli, S. A. Moiseev, B. C. Sanders, *Phys. Rev. A* **2012**, *85*, 050303(R).

[11] A. Nevet, N. Berkovitch, A. Hayat, P. Ginzburg, S. Ginzach, O. Sorias, M. Orenstein, *Nano Lett.* **2010**, *10*, 1848.

[12] S.-A. Biehs, G. S. Agarwal, *Phys. Rev. A* **2017**, *96*, 022308.

[13] P. Kok, W. J. Munro, K. Nemoto, T. C. Ralph, J. P. Dowling, G. J. Milburn, *Rev. Mod. Phys.* **2007**, *79*, 135.

[14] A. Vaziri, G. Weihs, A. Zeilinger, *Phys. Rev. Lett.* **2002**, *89*, 240401.

[15] S. Franke-Arnold, S. M. Barnett, M. J. Padgett, L. Allen, *Phys. Rev. A* **2002**, *65*, 033823.

[16] A. Davoyan, H. Atwater, *Optica* **2018**, *5*, 608.

[17] A. N. Poddubny, I. V. Iorsh, A. A. Sukhorukov, *Phys. Rev. Lett.* **2016**, *117*, 123901.

[18] S. Lan, L. Kang, D. T. Schoen, S. P. Rodrigues, Y. Cui, M. L. Brongersma, W. Cai, *Nat. Mater.* **2015**, *14*, 807.

[19] L. Liu, L. Wu, J. Zhang, Z. Li, B. L. Zhang, Y. Luo, *Adv. Sci.* **2018**, *5*, 1800661.

[20] T. Stav, A. Faerman, E. Maguid, D. Oren, V. Kleiner, E. Hasman, M. Segev, *Science* **2018**, *361*, 1101.

[21] K. Wang, J. G. Titchener, S. S. Kruk, L. Xu, H. P. Chung, M. Parry, I. I. Kravchenko, Y. H. Chen, A. S. Solntsev, Y. S. Kivshar, D. N. Neshev, A. A. Sukhorukov, *Science* **2018**, *361*, 1104.

[22] P. K. Jha, N. Shitrit, J. Kim, X. X. Ren, Y. Wang, X. Zhang, *ACS Photonics* **2018**, *5*, 971.

[23] S. Keren-Zur, O. Avayu, L. Michaeli, T. Ellenbogen, *ACS Photonics* **2016**, *3*, 117.

[24] G. X. Li, S. Chen, N. Pholchai, B. Reineke, P. W. H. Wong, E. Y. B. Pun, K. W. Cheah, T. Zentgraf, S. Zhang, *Nat. Mater.* **2015**, *14*, 607.

[25] Y. Q. Qin, C. Zhang, Y. Y. Zhu, X. P. Hu, G. Zhao, *Phys. Rev. Lett.* **2008**, *100*, 063902.

[26] Y. Ming, J. Tang, Z. X. Chen, F. Xu, L. J. Zhang, Y. Q. Lu, *IEEE J. Sel. Top. Quantum Electron.* **2015**, *21*, 6601206.

[27] N. Liu, H. Guo, L. Fu, S. Kaiser, H. Schweizer, H. Giessen, *Nat. Mater.* **2008**, *7*, 31.

[28] C. M. Soukoulis, M. Wegener, *Nat. Photonics* **2011**, *5*, 523.

[29] N. Segal, S. Keren-Zur, N. Hendler, T. Ellenbogen, *Nat. Photonics* **2015**, *9*, 180.

[30] U. Leonhardt, *Phys. Rev. A* **1993**, *48*, 3265.

[31] D. A. Antonosyan, A. S. Solntsev, A. A. Sukhorukov, *Photonics Res.* **2018**, *6*, A6.

[32] C. M. Caves, D. D. Crouch, *J. Opt. Soc. Am. B* **1987**, *4*, 1535.

[33] D. A. Antonosyan, A. S. Solntsev, A. A. Sukhorukov, *Phys. Rev. A* **2014**, *90*, 043845.

[34] Y. Ming, W. H. Zhang, Z. X. Chen, Z. J. Wu, J. Tang, F. Xu, L. J. Zhang, Y. Q. Lu, *ACS Photonics* **2016**, *3*, 2074.

[35] M. Decker, C. Kremers, A. Minovich, I. Staude, A. E. Miroshnichenko, D. Chigrin, D. N. Neshev, C. Jagadish, Y. S. Kivshar, *Opt. Express* **2013**, *21*, 8879.

[36] H. T. Chen, A. J. Taylor, N. F. Yu, *Rep. Prog. Phys.* **2016**, *79*, 076401.

[37] D. N. Vavulina, A. A. Sukhorukov, *Opt. Commun.* **2017**, *390*, 117.

[38] M. Gräfe, D. A. Antonosyan, A. S. Solntsev, A. A. Sukhorukov, A. Szameit, *Europhys. Lett.* **2017**, *118*, 54001.

[39] L. Allen, M. W. Beijersbergen, R. J. C. Spreeuw, J. P. Woerdman, *Phys. Rev. A* **1992**, *45*, 8185.

[40] A. Mair, A. Vaziri, G. Weihs, A. Zeilinger, *Nature* **2001**, *412*, 313.

[41] B. Y. Wei, W. Hu, Y. Ming, F. Xu, S. Rubin, J. G. Wang, V. Chigrinov, Y. Q. Lu, *Adv. Mater.* **2014**, *26*, 1590.

[42] L. L. Lu, P. Xu, M. L. Zhong, Y. F. Bai, S. N. Zhu, *Opt. Express* **2015**, *23*, 1203.

[43] F. M. Miatto, H. Di L. Pires, S. M. Barnett, M. P. Van Exter, *Eur. Phys. J. D* **2012**, *66*, 263.

[44] N. Nookala, J. Lee, M. Tymchenko, J. S. Gomez-Diaz, F. Demmerle, G. Boehm, G. Lai, G. Shvets, M. C. Amann, A. Alu, M. Belkin, *Optica* **2016**, *3*, 283.

[45] J. E. Sharping, K. F. Lee, M. A. Foster, A. C. Turner, B. S. Schmidt, M. Lipson, A. L. Gaeta, P. Kumar, *Opt. Express* **2006**, *14*, 12388.

[46] Y. M. Sua, J. Malowicki, M. Hirano, K. F. Lee, *Opt. Lett.* **2013**, *38*, 73.

[47] L. Shi, J. R. C. Andrade, A. Tajalli, J. Geng, J. Yi, T. Heidenblut, F. B. Segerink, I. Babushkin, M. Kholodtsova, H. Merdji, B. Bastiaens, M. Morgner, M. Kovacev, *Nano Lett.* **2019**, *19*, 4779.

[48] A. al Farooqui Md., J. Breeland, M. I. Aslam, M. Sadatgol, S. K. Özdemir, M. Tame, L. Yang, D. Ö. Güney, *Opt. Express* **2015**, *23*, 17941.

[49] M. Asano, M. Bechu, M. Tame, S. K. Özdemir, R. Ikuta, D. Ö. Güney, T. Yamamoto, L. Yang, M. Wegener, N. Imoto, *Sci. Rep.* **2016**, *5*, 18313.

[50] S. M. Wang, S. Y. Mu, C. Zhu, Y. X. Gong, P. Xu, H. Liu, T. Li, S. N. Zhu, X. Zhang, *Opt. Express* **2012**, *20*, 5213.

[51] B. Kante, Y. S. Park, K. O'Brien, D. Shuldman, N. D. Lanzillotti-Kimura1, Z. J. Wong, X. B. Yin, X. Zhang, *Nat. Commun.* **2012**, *3*, 1180.

[52] I. Bergmair, B. Dastmalchi, M. Bergmair, A. Saeed, W. Hilber, G. Hesser, C. Helgert, E. Pshenay-Severin, T. Pertsch, E. B. Kley, U. Hubner, N. H. Shen, R. Penciu, M. Kafesaki7, C. M. Soukoulis, K. Hingerl, M. Muehlberger, R. Schoeftner, *Nanotechnology* **2011**, *22*, 325301.

[53] M. L. Tseng, P. C. Wu, S. Sun, C. M. Chang, W. T. Chen, C. H. Chu, P. L. Chen, L. Zhou, D. W. Huang, T. J. Yen, D. P. Tsai, *Laser Photonics Rev.* **2012**, *6*, 702.

[54] D. Naidoo, F. S. Roux, A. Dudley, I. Litvin, B. Piccirillo, L. Marrucci, A. Forbes, *Nat. Photonics* **2016**, *10*, 327.

[55] J. W. Pan, Z. B. Chen, C. Y. Lu, H. Weinfurter, A. Zeilinger, M. Zukowski, *Rev. Mod. Phys.* **2012**, *84*, 777.

[56] J. S. Fakonas, H. Lee, Y. A. Kelaita, H. A. Atwater, *Nat. Photonics* **2014**, *8*, 317.

[57] J. Tang, Y. Ming, W. Hu, Y. Q. Lu, *Appl. Phys. Lett.* **2017**, *111*, 011105.

[58] Y. J. Lu, R. Sokhoyan, W. H. Cheng, G. K. Shirmanesh, A. R. Davoyan, R. A. Pala, K. Thyagarajan, H. A. Atwater, *Nat. Commun.* **2017**, *8*, 1631.

[59] C. Altuzarra, S. Vezzoli, J. Valente, W. Gao, C. Soci, D. Faccio, C. Couteau, *ACS Photonics* **2017**, *4*, 2124.

[60] A. Lyons, D. Oren, T. Roger, V. Savinov, J. Valente, S. Vezzoli, N. I. Zheludev, M. Segev, D. Faccio, *Phys. Rev. A* **2019**, *99*, 011801(R).

1900146 (8 of 8)